Magnetoentropic Signatures of the Textured Metamagnetic Phase of an Antiferromagnetic Polar Metal: $Ca_3Ru_2O_7$

Naoki Kikugawa[1]*, Dmitry A. Sokolov[2], Chanchal Sow[3,4], Yoshiteru Maeno[3], and Andrew Peter Mackenzie[2,5]

[1]*National Institute for Materials Science, 3-13 Sakura, Tsukuba, Ibaraki 305-0003, Japan*
[2]*Max Plank Institute for Chemical Physics of Solids, D-01187 Dresden, Germany*
[3]*Department of Physics, Kyoto University, Kyoto 606-8502, Japan*
[4]*Indian Institute of Technology, Kanpur 208016, Uttar Pradesh, India*
[5]*School of Physics and Astronomy, University of St. Andrews, St. Andrews KY16 9SS, United Kingdom*

(Received)

We report the magnetocaloric effect of a bilayered perovskite ruthenate $Ca_3Ru_2O_7$ that has recently been recognized as an antiferromagnetic polar metal. The magnetic entropy change obtained from temperature dependence of the DC magnetization measurements shows peaks and valleys under the magnetic field near metamagnetic transitions, and enable us to map out a thermodynamic field-temperature phase-diagram. The areas surrounded by the boundaries agree well with a novel "metamagnetic texture" with spin modulation observed recently by small angle neutron scattering measurements. We demonstrate that a thermodynamically equilibrium state is realized between the antiferromagnetic and spin-polarized states throughout the metamagnetic transition in this polar metal.

The Ruddlesden-Popper type bilayered-ruthenate $Ca_3Ru_2O_7$ has attracted much attention because of rich physical properties linked to a polar crystal structure belonging to the space group $Bb2_1m$ [1,2]. The crystal structure presented in Fig. 1 consists of RuO_2 bilayers along the crystallographic *c* axis with corner-sharing RuO_6 octahedra. The octahedra of $Ca_3Ru_2O_7$ are rotated around by the *c* axis and tilted with respect to the *ab* plane. Consequently, the structure globally breaks inversion symmetry with the polar direction along the *b* axis [3]. The material displays multiple transitions on cooling [1]: one is an antiferromagnetic order at the transition temperature (T_N) of 56 K, where the ordered moments align along the *a* axis, and the propagation vector runs along the *c* axis. The moments are coupled ferromagnetically within

the bilayer, while antiferromagnetic coupling is formed between the adjacent bilayers. The other is a spin-reorientation transition at 48 K (T_S) together with a first-order isostructural transition leading to a compression of the crystal structure along the *c* axis. Below T_S, the magnetically ordered moments align to the *b* axis but the coupling between the adjacent bilayers remains antiferromagnetic [1]. The isothermal magnetization at low temperatures exhibits a localized metamagnetic transition when the field is applied along the in-plane direction. The metamagnetism under the field along *b* axis is presented in Fig. 2. The saturated moment at high fields reaches nearly the full moment (2 μ_B) of Ru^{4+} under the low spin configuration in the t_{2g} state [4].

The electronic structure of this material has also been recognized to be intriguing because it strongly couples to the above magnetic order [5]. Below T_S, angle-resolved photoemission-spectroscopy measurements revealed an electron (a hole) pocket at the boundary of Brillouin zone along k_x (k_y) direction, but the pocket occupies only 0.3% of the zone [5–7]. The observed small Fermi-surfaces are consistent with quantum oscillation and magneto-transport measurements [8–10]. These hole- and electron-pockets are attributed to in-plane anisotropy due to the orthorhombicity of the crystal structure [9]. In addition, a renormalized "M-shaped" dispersion gapped around the zone center starts to cross the Fermi energy above T_S, and a hole-like Fermi-surface around the Γ point occupies nearly half of the zone [5,6]. The gap opening around the Γ point below T_S can be explained in terms of the band hybridization mediated by a Rashba-type spin-orbit coupling. The coupling is activated when the spin reorientation to the *b* axis is perpendicular to the potential at the Ru site induced by the symmetry-breaking [5]. Thus, the interplay between the spin-orbit coupling and electronic correlations drives such a drastic reconstruction of the electronic structure. Significantly, this system is an "antiferromagnetic polar metal" reflecting the conducting nature under the non-centrosymmetric structure of $Bb2_1m$ across T_S.

Very recently, motivated by the above physical properties in this noncentrosymmetric material, a novel "metamagnetic texture" with a spin modulation along the *a* axis has been revealed using small-angle neutron scattering (SANS) when a magnetic field is applied to the *b* axis [11]. Here, modulation with a period ranging from 8 and 20 nm is seen in a limited field-temperature region: in the temperature (*T*) range between 42 and 52 K, and the field (*H*) range between 2 and 5 T. The field-induced metamagnetic texture as an equilibrium state developing between the antiferromagnetic and polarized state is ascribable to the asymmetric Dzyaloshinskii-Moriya exchange interactions originating from the distorted crystal structure.

The finding of the metamagnetic texture reminds us of chiral skyrmion phases seen in several B20 series ferrimagnets [12–14], and the particle-like condensed states provide a rich phase diagram determined by several experimental techniques. In $Ca_3Ru_2O_7$, the nature of the metamagnetic texture has also been investigated by means of electrical transport measurement [11]; however, detailed thermodynamic properties of the observed texture have remained unclear. To clarify this, the magnetocaloric effect is a desirable tool to derive a magnetic entropy change at the phase boundaries, as was successful in $Sr_3Ru_2O_7$ by studying the change of sample temperature with magnetic field [15]. Equivalent information can be derived from DC magnetization measurements using the thermodynamic relation $\left(\frac{\partial S}{\partial \mu_0 H}\right)_T = \left(\frac{\partial M}{\partial T}\right)_{\mu_0 H}$, where S is the entropy, μ_0 the magnetic permeability in vacuum, H the magnetic field, M the magnetization, and T the temperature [16]. In this paper, we report the magnetocaloric effect of this material with a focus on an entropy gain/release at the phase boundaries.

Single crystals of $Ca_3Ru_2O_7$ were grown using a floating-zone technique in optical two-mirror furnaces in Kyoto and Dresden (Canon Machinery Inc., SC-K15HD, and SCI-MDH, respectively). The crystals were grown in an atmosphere of the mixture gas of Ar and O_2 with the ratio of Ar : O_2 = 85 : 15 or 90 : 10. The growth speed was typically 7-8 mm/h [11]. The as-grown crystals were oriented using the X-ray Laue back-scattering method. The temperature (T) dependence of the DC magnetization (M) was measured with increasing temperature under fixed field using superconducting quantum interference device magnetometers (MPMS and VSM, Quantum Design) under magnetic fields of up to 7 T. Here, the field was applied along the b axis, and the measurements were performed under the field-cooled protocol. The field interval of the M-T measurement was 0.25 T for Sample #1 with the mass of 1.53 mg, and 0.05 T for Sample #2 with the mass of 0.37 mg. The magnetic entropy change (ΔS) is obtained by $\Delta S(T, \Delta\mu_0 H) = \int^{\Delta\mu_0 H} \left(\frac{\partial M}{\partial T}\right)_{\mu_0 H'} d(\mu_0 H') \approx \left(\frac{M(T+\Delta T)-M(T)}{\Delta T}\right) \times \Delta(\mu_0 H)$, where $\Delta(\mu_0 H)$ is the field interval. We note that the reported ΔS for magnetic materials was typically obtained from zero to 5 T in order to evaluate the performance of the magnetocaloric effect between the demagnetized (0 T) and magnetized (5 T) process [17]. However, in this study, we evaluated the ΔS of $Ca_3Ru_2O_7$ under the field interval of $\Delta(\mu_0 H)$ = 0.25 T (Sample #1), and 0.05 T (Sample #2) in order to see the entropy change at the phase boundary of, in particular, the steep magnetization change caused by the metamagnetism. Although we show the entropy change of sample #2 (Fig. 5) measured under the narrower field intervals, the overall tendency obtained

in sample #1 was similar.

In Fig. 3, we show the temperature dependence of the magnetization of $Ca_3Ru_2O_7$ under fields of up to 7 T. At high temperatures, a typical Curie-Weiss-like behavior is seen. Here, the effective moment ($\mu_{\rm eff}$) from the Curie-Weiss fit corresponds to $S = 1$, consistent with the low spin configuration of Ru^{4+} ($4d^4$). When the applied field is lower, the value of the magnetization is low at low temperatures reflecting the antiferromagnetic ordered state. An abrupt jump of the magnetization is observed, reflecting the first-order phase transition [1]. The jump shifts to lower temperature with increasing field, and cusp-like behavior is seen around 50 K at intermediate fields (2.5 – 4.5 T). The behavior at low temperature changes dramatically above 6 T: the magnetization at the lowest temperature measured reaches nearly 2 μ_B, corresponding to the fully polarized state. The sudden change of the magnetization between 5.5 and 6 T represents a localized metamagnetic transition. The magnetization is suppressed with increasing temperature with a step-like behavior around 45 K, indicating the existence of a magnetic structure when the magnetic behavior crossovers from spin-polarized to paramagnetic state under high field.

Figure 4 shows temperature derivatives of the magnetization (dM/dT) as a function of temperature at representative fields for Sample #1. At 2 T (Fig. 3(a)), the peak and inflection in dM/dT correspond to the transitions at T_S and T_N, respectively. With increasing field, an additional valley with a negative sign of dM/dT appears just above T_S, and the valley shifts to higher temperature with field (Figs. 3(b) – (f)). On the other hand, the positive peak corresponding to T_S shifts to lower temperatures. Finally, at 6 T, where the metamagnetic transition sets in, two valleys with negative signs are observed in the dM/dT over the whole temperature range. The dM/dT directly represents the field derivatives of the entropy, $dS/d(\mu_0 H)$. Considering the relation $C/T = dS/dT$, where C is the specific heat, the peaks and valleys in $dS/d(\mu_0 H)$ imply field-induced first-order phase transitions with heat absorption and release, respectively. We note that the region between the peak and the valley in dM/dT represents the area of the metamagnetic texture seen in SANS as described below.

Figure 5 displays a contour map of ΔS evaluated under the field interval $\Delta(\mu_0 H) = 0.05$ T calculated from the dM/dT. We can clearly identify several phase boundaries: (i) a sharp $\Delta S > 0$ for $T < 48$ K and $\mu_0 H < 5$ T, (ii) a sharp $\Delta S < 0$ for 48 K $< T <$ 51 K and 2 T $< \mu_0 H <$ 3.5 T, (iii) a sharp $\Delta S < 0$ for $T > 42$ K and $\mu_0 H > 5.5$ T, and (iv) a faint but clear $\Delta S < 0$ for $48 < T <$ 53 K and 3 T $< \mu_0 H <$ 5.5 T. The boundary (i) at which heat is absorbed corresponds to the first-

order structural transition at T_S. In contrast, the boundaries (ii), (iii), and (iv) release heat. Interestingly, the area surrounded by the phase boundaries (i) – (iv) correspond well to the observed "metamagnetic signature" region [11]. Inside that region the entropy is lower (-0.02 J/mol K). This is in contrast to the skyrmion system in several ferrimagnetic systems stabilized by thermal fluctuations, in which the skyrmion phase shows higher entropy than other phases in the field-temperature phase-diagram [12–14]. The difference might reflect that the "metamagnetic texture" in $Ca_3Ru_2O_7$ appears between the antiferromagnetic and spin-polarized states via a localized metamagnetic transition [11], whereas the skyrmion lattice appears between conical phases. It is worth attempting to apply the thermodynamic Clausius-Clapeyron relation $d(\mu_0 H_c)/dT = -\Delta S/\Delta M$ to the phase boundary (iv), since the newly detected boundary in the thermodynamic probe (magnetization in this study) is relatively faint, and it has been discussed in terms of a "crossover" following analysis of transport measurements [18]. Here $\mu_0 H_c$ is the critical field along the boundary (iv). Considering the magnetization jump (ΔM) with 0.05 μ_B/Ru, and $d(\mu_0 H)/dT \sim +2.3$ T/K at $T = 51$ K, we obtain an entropy change of –13 mJ/mol K. This is in fairly good agreement with the value of –17 mJ/mol K obtained from the Maxwell relation from the M-T curves, including the sign of ΔS. This provides evidence for a phase transition, and hence that the region of the metamagnetic texture with the modulated spin-structure can be defined as a thermodynamic phase.

We finally mention that although we argue the phase boundaries that we have observed correspond to the "metamagnetic texture" revealed by the SANS measurements [11], a recent resonant X-ray scattering measurement has reported an incommensurate cycloidal phase [19]. Here, the incommensurability is essentially consistent with the SANS result, but such a phase would persist down to the zero field. Also, the faint but clear phase boundary (iv) revealed in our study has not been detected. Although the discrepancies between the results obtained using different experimental techniques are currently an open question, we note that the system is very sensitive to disorder and substitution. A metal-insulator transition occurs under a tiny substitution of 0.2% nonmagnetic Ti, triggered by a drastic change of the valence band [20]. Also, substitution raises both the transition temperatures (T_N and T_S), and modifies the magnetic structure [21]. Thus, the system is located at a delicate balance point at the boundary between metal and insulator.

In summary, we have deduced the magnetocaloric effect of an antiferromagnetic polar metal $Ca_3Ru_2O_7$ from measurements of the DC magnetization. The peaks and valleys of the magnetic

entropy change correspond to phase boundaries, and the area surrounded by the boundaries agrees well with that in which “metamagnetic texture” has been observed by SANS measurements. We therefore confirm that the “metamagnetic texture” is a thermodynamic equilibrium state realized between the antiferromagnetic and spin-polarized state throughout the metamagnetic transition of this polar metal. $Ca_3Ru_2O_7$ therefore provides a rich opportunity to explore the underlying physics of the interplay between spin-orbit coupling and electronic correlations which are strongly influenced by disorder, and merits further experimental and theoretical study.

Acknowledgments

We acknowledge Takanobu Hiroto for valuable discussion. This work is supported by a KAKENHI Grants-in-Aids for Scientific Research (Grant Nos. 17H06136, 18K04715, and 21H01033), and Core-to-Core Program (No. JPJSCCA20170002) from the Japan Society for the Promotion of Science (JSPS) and by a JST-Mirai Program (Grant No. JPMJMI18A3).

*E-mail: KIKUGAWA.Naoki@nims.go.jp

References

[1] Y. Yoshida, S.-I. Ikeda, H. Matsuhata, N. Shirakawa, C. H. Lee, and S. Katano, *Crystal and magnetic Structure of $Ca_3Ru_2O_7$*, Phys. Rev. B **72**, 054412 (2005). https://doi.org/10.1103/physrevb.72.054412

[2] S. Lei, M. Gu, D. Puggioni, G. Stone, J. Peng, J. Ge, Y. Wang, B. Wang, Y. Yuan, K. Wang, Z. Mao, J. M. Rondinelli, and V. Gopalan, *Observation of Quasi-two-dimensional polar domains and ferroelastic switching in a metal, $Ca_3Ru_2O_7$*, Nano Lett. **18**, 3088 (2018). https://doi.org/10.1021/acs.nanolett.8b00633

[3] E. A. Nowadnick and C. J. Fennie, *Domains and Ferroelectric switching pathways in $Ca_3Ti_2O_7$ from first principles*, Phys. Rev. B **94**, 104105 (2016). https://doi.org/10.1103/physrevb.94.104105

[4] E. Ohmichi, Y. Yoshida, S. I. Ikeda, N. Shirakawa, and T. Osada, *Colossal magnetoresistance accompanying a structural transition in a highly two-dimensional metallic state of $Ca_3Ru_2O_7$*, Phys. Rev. B **70**, 104414 (2004). https://doi.org/10.1103/physrevb.70.104414

[5] I. Marković, M. D. Watson, O. J. Clark, F. Mazzola, E. Abarca Morales, C. A. Hooley, H. Rosner, C. M. Polley, T. Balasubramanian, S. Mukherjee, N. Kikugawa, D. A. Sokolov, A. P. Mackenzie, and P. D. C. King, *Electronically driven spin-reorientation transition of the correlated polar metal $Ca_3Ru_2O_7$*, Proc. Natl. Acad. Sci. U.S.A. **117**, 15524 (2020). https://doi.org/10.1073/pnas.2003671117

[6] M. Horio, Q. Wang, V. Granata, K. P. Kramer, Y. Sassa, S. Jöhr, D. Sutter, A. Bold, L. Das, Y. Xu, R. Frison, R. Fittipaldi, T. K. Kim, C. Cacho, J. E. Rault, P. Le Fèvre, F. Bertran, N. C. Plumb, M. Shi, A. Vecchione, M. H. Fischer, and J. Chang, *Electron-driven C_2-symmetric Dirac semimetal uncovered in $Ca_3Ru_2O_7$*, npj Quantum Materials **6**, 29 (2021). https://doi.org/10.1038/s41535-021-00328-3

[7] F. Baumberger, N. J. C. Ingle, N. Kikugawa, M. A. Hossain, W. Meevasana, R. S. Perry, K. M. Shen, D. H. Lu, A. Damascelli, A. Rost, A. P. Mackenzie, Z. Hussain, and Z.-X. Shen, *Nested Fermi surface and electronic instability in $Ca_3Ru_2O_7$*, Phys. Rev. Lett. **96**, 107601 (2006). https://doi.org/10.1103/PhysRevLett.96.107601

[8] Y. Yoshida, I. Nagai, S.-I. Ikeda, N. Shirakawa, M. Kosaka, and N. Môri, *Quasi-two-dimensional metallic ground state of $Ca_3Ru_2O_7$*, Phys. Rev. B **69**, 220411 (2004). https://doi.org/10.1103/physrevb.69.220411

[9] N. Kikugawa, A. W. Rost, C. W. Hicks, A. J. Schofield, and A. P. Mackenzie, *$Ca_3Ru_2O_7$: Density wave formation and quantum oscillations in the Hall Resistivity*, J. Phys. Soc. Jpn. **79**, 024704 (2010). https://doi.org/10.1143/JPSJ.79.024704

[10] L. Das, Y. Xu, T. Shang, A. Steppke, M. Horio, J. Choi, S. Jöhr, K. von Arx, J. Mueller, D. Biscette, X. Zhang, A. Schilling, V. Granata, R. Fittipaldi, A. Vecchione, and J. Chang, *Two-carrier magnetoresistance: applications to $Ca_3Ru_2O_7$*, J. Phys. Soc. Jpn. **90**, 054702 (2021). https://doi.org/10.7566/JPSJ.90.054702

[11] D. A. Sokolov, N. Kikugawa, T. Helm, H. Borrmann, U. Burkhardt, R. Cubitt, J. S. White, E. Ressouche, M. Bleuel, K. Kummer, A. P. Mackenzie, and U. K. Rößler, *Metamagnetic texture in a polar antiferromagnet*, Nat. Phys. **15**, 671 (2019).
https://doi.org/10.1038/s41567-019-0501-0

[12] A. Bauer, M. Garst, and C. Pfleiderer, *Specific heat of the skyrmion lattice phase and field-induced tricritical point in MnSi*, Phys. Rev. Lett. **110**, 177207 (2013).
https://doi.org/10.1103/PhysRevLett.110.177207

[13] J. D. Bocarsly, R. F. Need, R. Seshadri, and S. D. Wilson, *Magnetoentropic signatures of skyrmionic phase behavior in FeGe*, Phys. Rev. B **97**, 100404 (2018).
https://doi.org/10.1103/PhysRevB.97.100404

[14] C. Dhital and J. F. DiTusa, *Entropic signatures of the skyrmion lattice phase in $MnSi_{1-x}Al_x$ and $Fe_{1-y}Co_ySi$*, Phys. Rev. B **102**, 224408 (2020).
https://doi.org/10.1103/PhysRevB.102.224408

[15] A. W. Rost, R. S. Perry, J.-F. Mercure, A. P. Mackenzie, and S. A. Grigera, *Entropy landscape of phase formation associated with quantum criticality in $Sr_3Ru_2O_7$*, Science **325**, 1360 (2009).
https://doi.org/10.1126/science.1176627

[16] V. K. Pecharsky, K. A. Gschneidner, A. O. Pecharsky, and A. M. Tishin, *Thermodynamics of the magnetocaloric effect*, Phys. Rev. B **64**, 144406 (2001).
https://doi.org/10.1103/PhysRevB.64.144406

[17] K. A. Gschneidner and V. K. Pecharsky, *Magnetocaloric Materials*, Annu. Rev. Mater. Sci. **30**, 387 (2000).
https://doi.org/10.1146/annurev.matsci.30.1.387

[18] D. Fobes, J. Peng, Z. Qu, T. J. Liu, and Z. Q. Mao, *Magnetic phase transitions and bulk spin-valve effect tuned by in-plane field orientation in $Ca_3Ru_2O_7$*, Phys. Rev. B **84**, 014406 (2011).
https://doi.org/10.1103/PhysRevB.84.014406

[19] C. D. Dashwood, L. S. I. Veiga, Q. Faure, J. G. Vale, D. G. Porter, S. P. Collins, P. Manuel, D. D. Khalyavin, F. Orlandi, R. S. Perry, R. D. Johnson, and D. F. McMorrow, *Spontaneous cycloidal order mediating a spin-reorientation transition in a polar metal*, Phys. Rev. B **102**, 180410 (2020).
http://dx.doi.org/10.1103/PhysRevB.102.180410

[20] S. Tsuda, N. Kikugawa, K. Sugii, S. Uji, S. Ueda, M. Nishio, and Y. Maeno, *Mott Transition Extremely Sensitive to Impurities in $Ca_3Ru_2O_7$ revealed by Hard X-Ray Photoemission Studies*, Phys. Rev. B **87**, 241107 (2013).
https://doi.org/10.1103/physrevb.87.241107

[21] X. Ke, J. Peng, D. J. Singh, T. Hong, W. Tian, C. R. Dela Cruz, and Z. Q. Mao, *Emergent Electronic and Magnetic State in $Ca_3Ru_2O_7$ induced by Ti Doping*, Phys. Rev. B Condens. Matter Mater. Phys. **84**, (2011).
https://doi.org/10.1103/physrevb.84.201102

Figure captions

Figure 1 (Color online)

(a) Crystal structure of a bilayered ruthenate $Ca_3Ru_2O_7$ with a space group of $Bb2_1m$. The dotted lines represent the unit cell. The crystal view from (b) *a* axis, (c) *b* axis, and (d) *c* axis after omitting Ca atoms. The structure globally breaks inversion symmetry with the polar direction along the *b* axis as a consequence of the rotating octahedra around by the *c* axis and tilting with respect to the *ab* plane. (e) The view from the *c* axis together with the in-plane oxygen O3 and O4 and their inversion symmetry operation from (*x*, *y*, *z*) to (-*x*, -*y*, -*z*) presented as O3' and O4', respectively. Since the system breaks inversion symmetry, O3 and O4 do not overlap with O3' and O4'.

Figure 2 (Color online)

Isothermal magnetization of $Ca_3Ru_2O_7$ under the magnetic field along the *b* axis. The magnetization presented here is particularly focused on the temperature region at which the "metamagnetic texture" is observed. This is in sharp contrast to the single sharp transition at 2 K.

Figure 3 (Color online)

Temperature dependence of the magnetization of $Ca_3Ru_2O_7$ up to 7 T. The data were taken with increasing temperature under field-cooled process.

Figure 4 (Color online)

Temperature derivatives of the magnetization (*dM/dT*) as a function of temperature at representative fields.

Figure 5 (Color)

Contour map of the magnetic entropy change ΔS under applying the field along *b* axis. Here, the magnetic entropy change ΔS was evaluated under the field interval $\Delta(\mu_0 H) = 0.05$ T from the *dM/dT*.

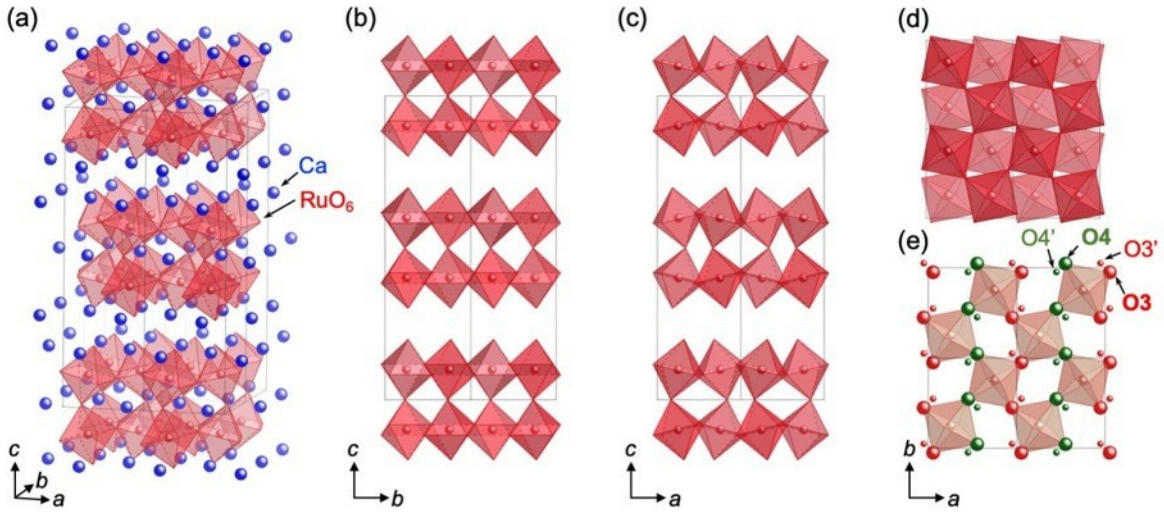

Fig. 1

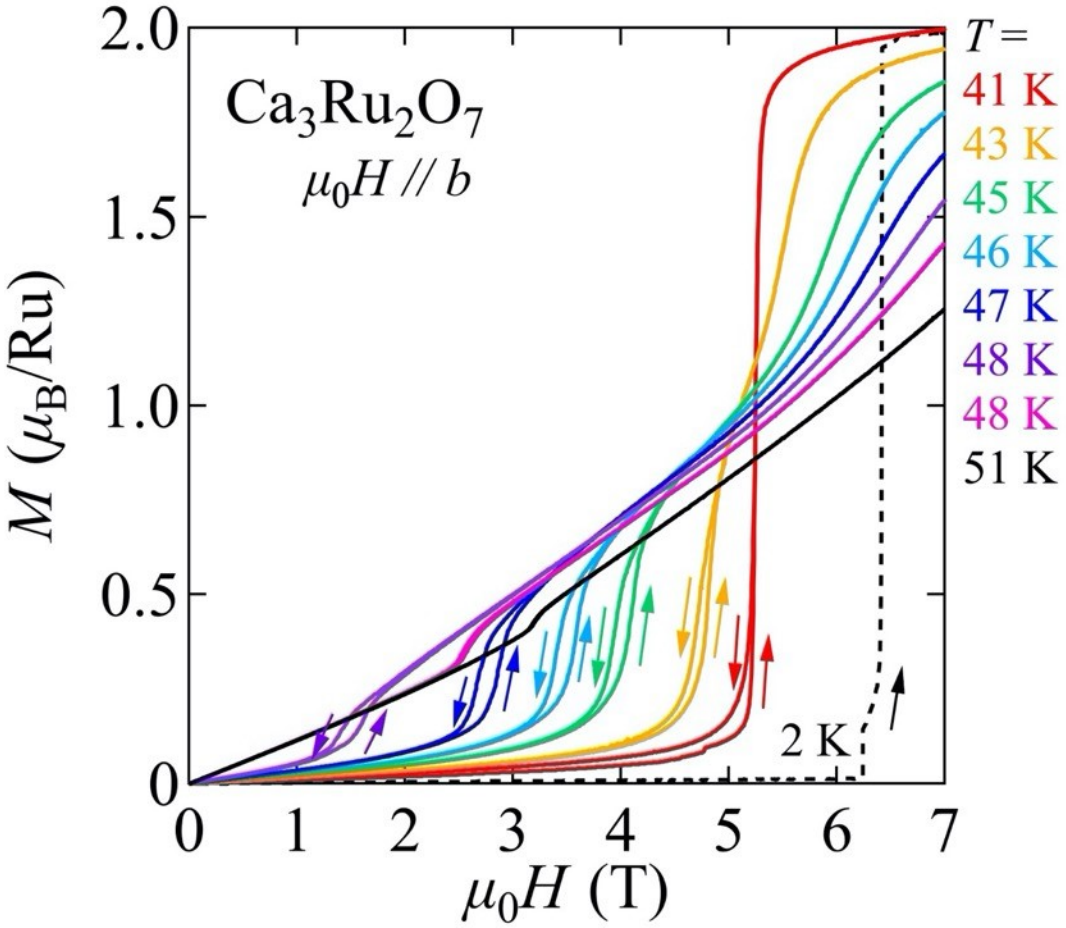
2.0
1.5
1.0
0.5
0
0
1
2
3
4
5
6
7
M (μ_B/Ru)
$\mu_0 H$ (T)
$Ca_3Ru_2O_7$
$\mu_0 H$ // b
T =
41 K
43 K
45 K
46 K
47 K
48 K
48 K
51 K
2 K

Fig. 2

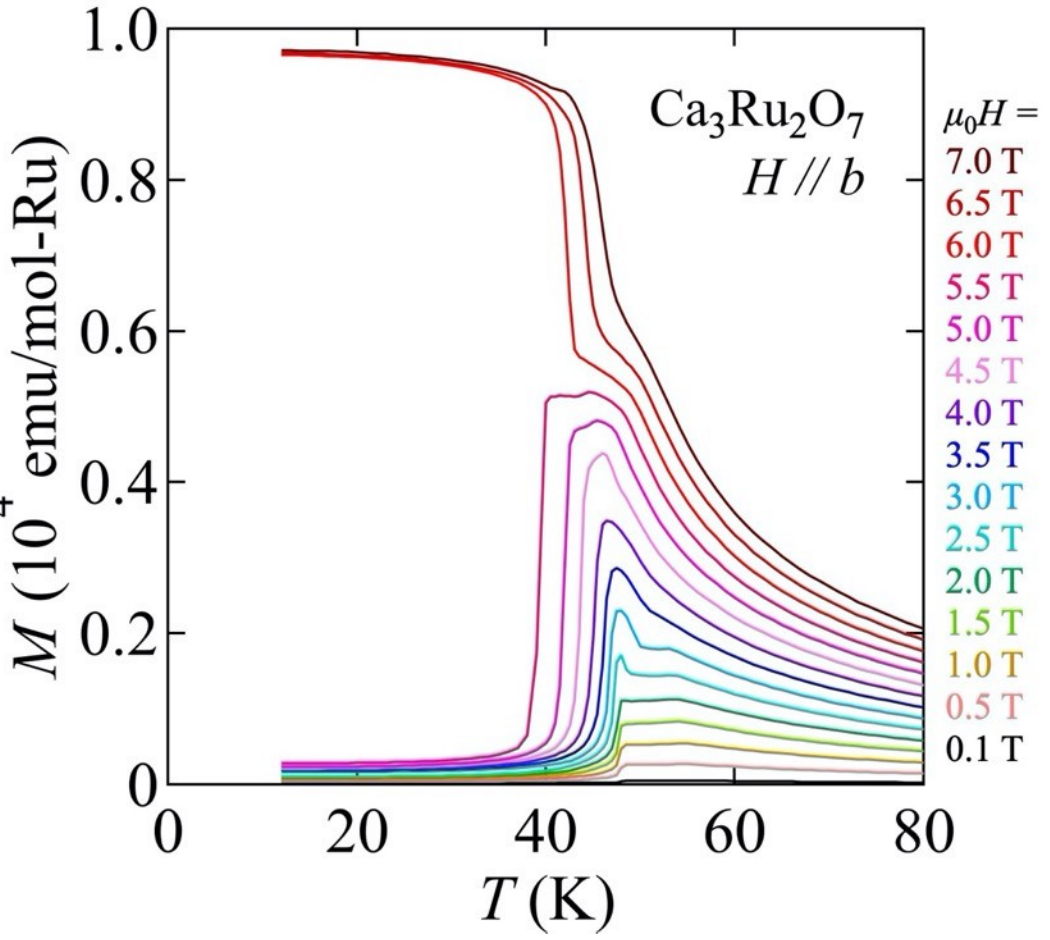
1.0
0.8
0.6
0.4
0.2
0
0
20
40
60
80
M (10^4 emu/mol-Ru)
T (K)
Ca3Ru2O7
H // b
μ0H =
7.0 T
6.5 T
6.0 T
5.5 T
5.0 T
4.5 T
4.0 T
3.5 T
3.0 T
2.5 T
2.0 T
1.5 T
1.0 T
0.5 T
0.1 T

Fig. 3

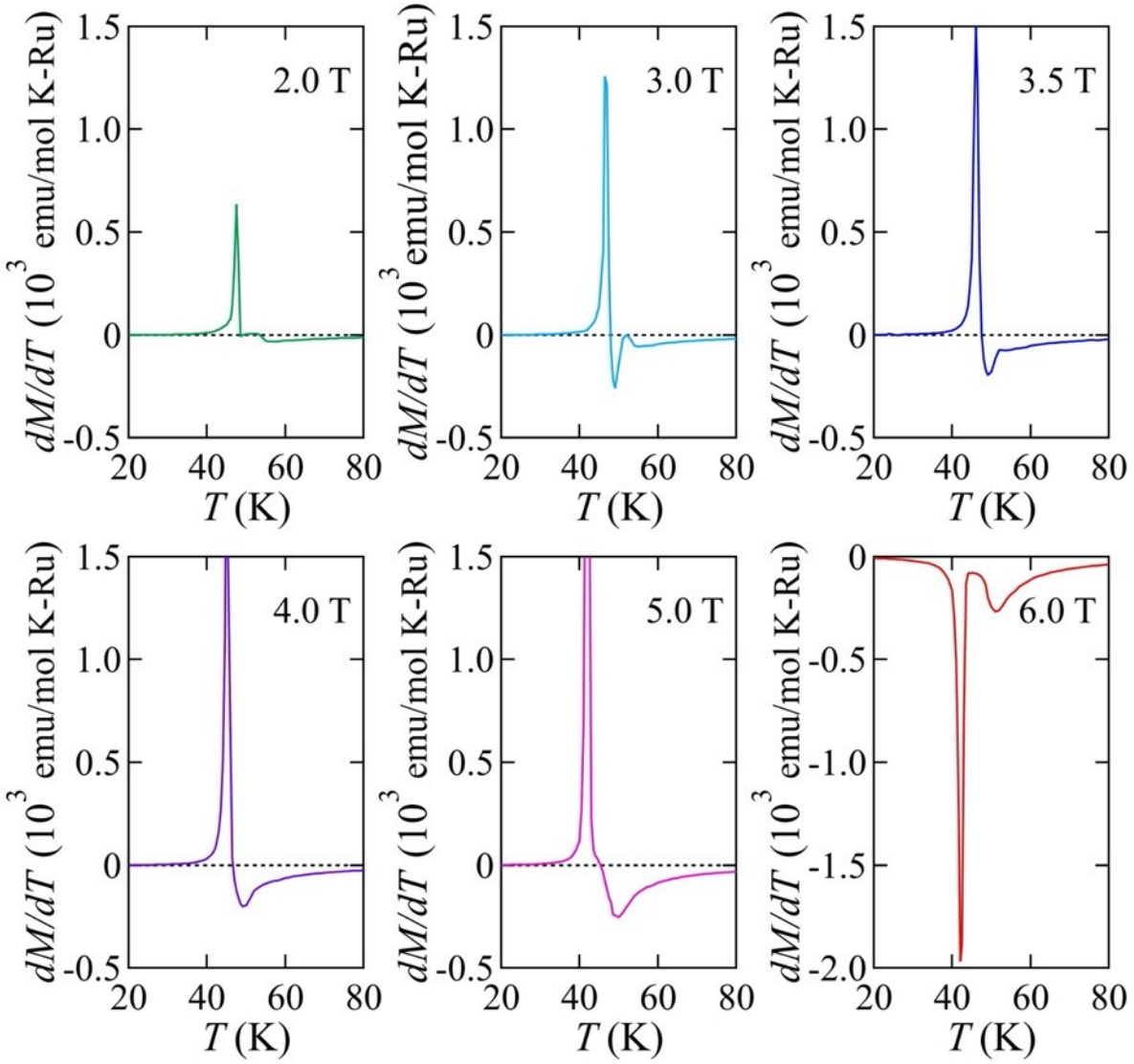

Fig. 4

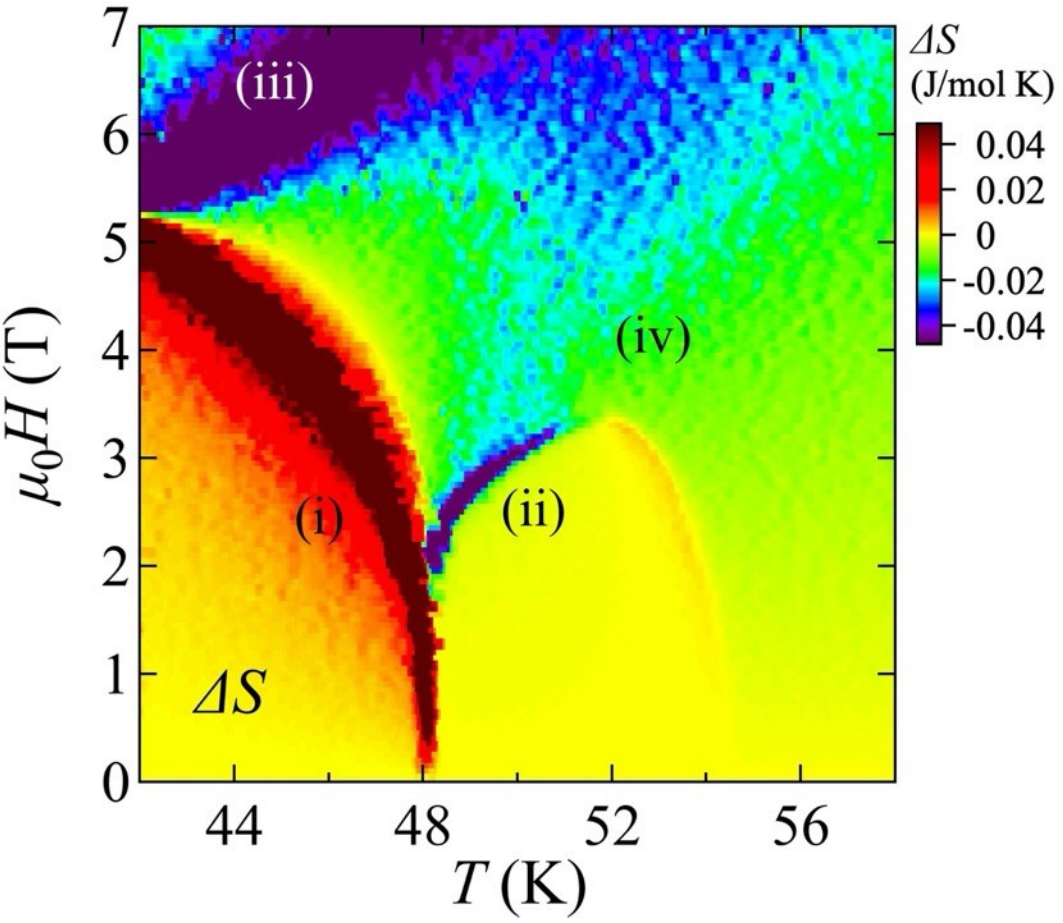
(iii)
(iv)
(i)
(ii)
ΔS
ΔS
(J/mol K)
0.04
0.02
0
-0.02
-0.04
μ0H (T)
T (K)
0
1
2
3
4
5
6
7
44
48
52
56

Fig. 5